Supporting Information

Impact of Fabrication Methods on Binder Distribution and Charge Transport in Composite Cathodes of All-Solid-State Batteries

Benjamin Emley[1,†], Chaoshan Wu[1,†], Lihong Zhao[1,2], Qing Ai[3], Yanliang Liang[1,2], Zhaoyang Chen[1], Liqun Guo[1], Tanguy Terlier[4], Jun Lou[3], Zheng Fan[5,*], Yan Yao[1,2,*]

Table S1 Relevant numbers for calculating the ionic and electronic conductivities from electrical impedance spectroscopy and DC polarization evaluations of composite cathodes shown in Fig. 4c and 4e, respectively.

		Thickness (cm)	$Z_{solid\ electrolyte}$ (Ohm)	$Z_{cathode}$ (Ohm)	EIS fitting accuracy χ^2	$\sigma_{ionic,\ CC}$ (S cm^{-1})	$\sigma_{electronic,\ CC}$ (S cm^{-1})
30 °C	Wet, 0.5 wt.% NBR	3.0×10^{-3}	255	167	2.6×10^{-4}	3.3×10^{-6}	3.0×10^{-3}
	Dry, 0.5 wt% PTFE	8.9×10^{-3}	544	105	1.2×10^{-3}	6.9×10^{-5}	4.6×10^{-2}
	Dry, 0.5 wt.% PTFE solvent treated SE	6.6×10^{-3}	533	493	2.4×10^{-4}	1.3×10^{-5}	7.6×10^{-2}
45 °C	Wet, 0.5 wt.% NBR	3.0×10^{-3}	158	106	2.8×10^{-4}	5.4×10^{-6}	2.2×10^{-3}
	Dry, 0.5 wt% PTFE	8.9×10^{-3}	259	52	1.3×10^{-3}	1.4×10^{-4}	4.2×10^{-2}
	Dry, 0.5 wt.% PTFE solvent treated SE	6.6×10^{-3}	250	307	2.0×10^{-4}	2.8×10^{-5}	7.3×10^{-2}
60 °C	Wet, 0.5 wt.% NBR	3.0×10^{-3}	81	62	1.3×10^{-3}	7.8×10^{-6}	1.0×10^{-3}
	Dry, 0.5 wt% PTFE	8.9×10^{-3}	137	28	1.5×10^{-3}	2.5×10^{-4}	4.1×10^{-2}
	Dry, 0.5 wt.% PTFE solvent treated SE	6.6×10^{-3}	116	213	1.7×10^{-4}	6.2×10^{-5}	6.7×10^{-2}
75 °C	Wet, 0.5 wt.% NBR	3.0×10^{-3}	40	33	1.0×10^{-3}	1.1×10^{-5}	6.3×10^{-4}
	Dry, 0.5 wt% PTFE	8.9×10^{-3}	78	18	1.3×10^{-3}	3.9×10^{-4}	3.5×10^{-2}
	Dry, 0.5 wt.% PTFE solvent treated SE	6.6×10^{-3}	73	162	7.7×10^{-4}	9.6×10^{-5}	5.6×10^{-2}

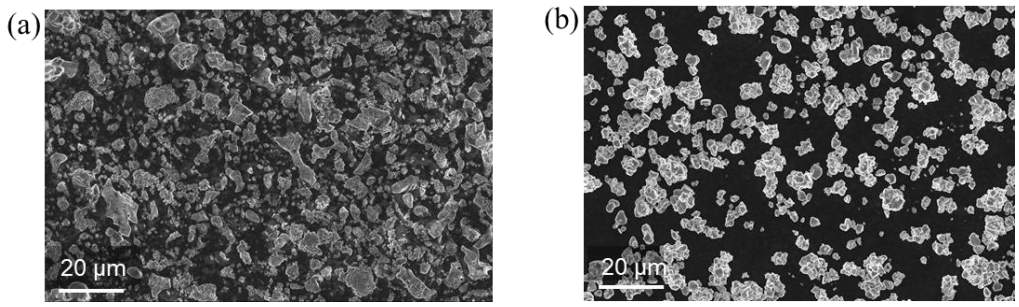

Fig. S1 SEM images of pristine (a) Li_6PS_5Cl particles and (b) single-crystal NMC powdes used in the composite cathode.

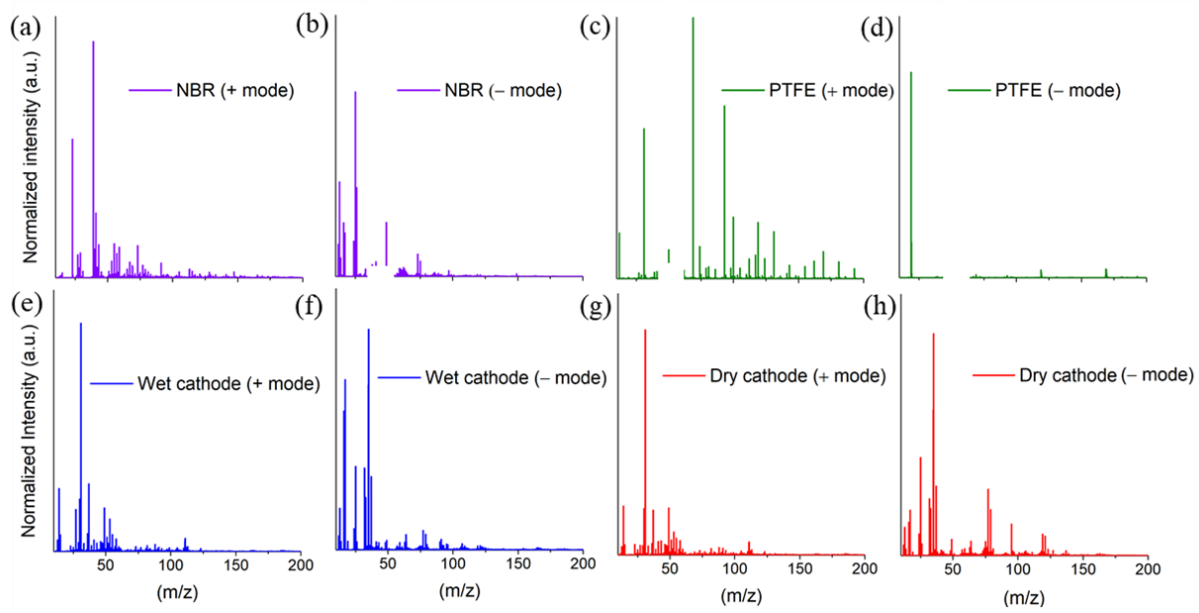

Fig. S2 Normalized intensities vs. mass to charge ratio from TOF-SIMS of the negative and positive modes for (a, b) nitrile butadiene rubber, (c, d) polytetrafluoroethylene, and the composite cathodes prepared via (e, f) the wet process and (g, h) dry process.

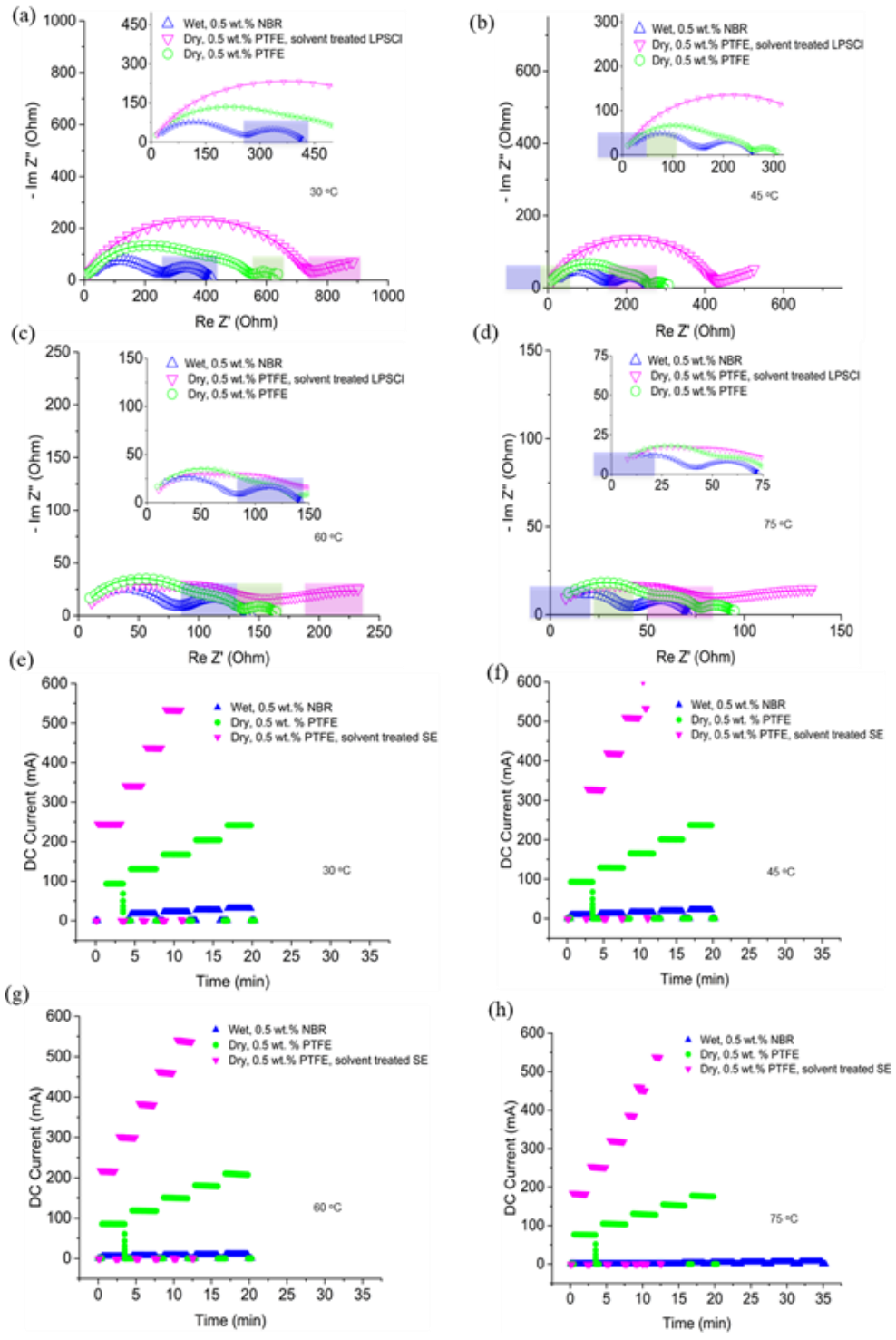

Fig. S3 Measurements of ionic and electronic conductivity of composite cathodes. (a-d) Electrical impedance spectroscopy of composite cathodes at different temperatures as indicated with the 3rd depressed semi-circle highlighted representing the contribution of the ionic conductivity of the composite cathode. (e-h) DC polarization measurements of the same composite cathodes to determine its electronic conductivity.

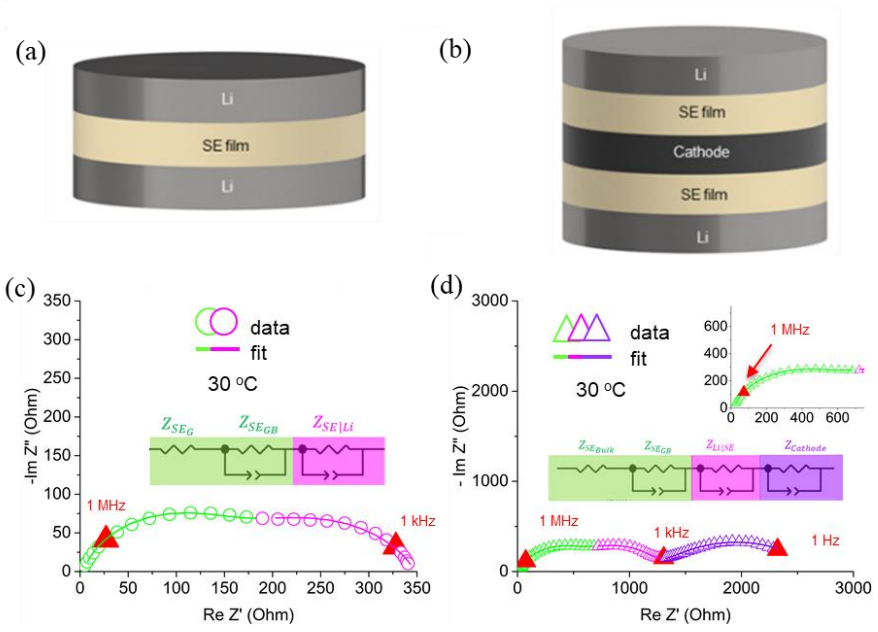

Fig. S4 Electrochemical impendance spectra menasurements and equivalent circuit models for two representative samples. (a-b) A symmetrical cell with a Li | SE | Li configuration, displaying two depressed semi-circles. (c-d) A symmetrical cell with a Li | SE | composite cathode | SE | Li configuration, exhibiting an additional, depressed semi-circle that represents the contribution of the cathode composite.

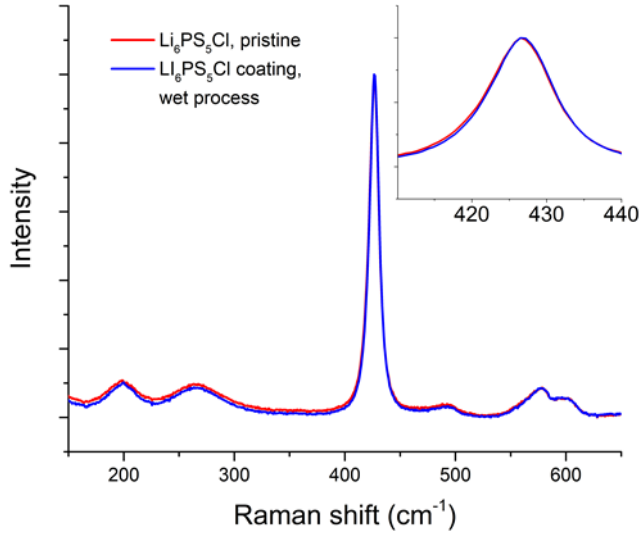

Fig. S5 Raman spectra of Li_6PS_5Cl in the form of a pellet prepared from pristine powder and within a coating prepared with 5 wt.% polymer binder using a wet coating process; the inset focuses on the region near 428 cm^{-1}, commonly attributed to a vibrational mode of the covalently bonded, tetrahedral PS_4^{3-}.